Dalton Transactions

An international journal of inorganic chemistry

## Accepted Manuscript

This article can be cited before page numbers have been issued, to do this please use: Y. Lai, X. Wang, R. Dai, Y. Huang, X. Zhou, X. Zhou and D. Li, *Dalton Trans.*, 2020, DOI: 10.1039/D0DT01340D.


This is an Accepted Manuscript, which has been through the Royal Society of Chemistry peer review process and has been accepted for publication.

Accepted Manuscripts are published online shortly after acceptance, before technical editing, formatting and proof reading. Using this free service, authors can make their results available to the community, in citable form, before we publish the edited article. We will replace this Accepted Manuscript with the edited and formatted Advance Article as soon as it is available.

You can find more information about Accepted Manuscripts in the Information for Authors.

Please note that technical editing may introduce minor changes to the text and/or graphics, which may alter content. The journal's standard Terms & Conditions and the Ethical guidelines still apply. In no event shall the Royal Society of Chemistry be held responsible for any errors or omissions in this Accepted Manuscript or any consequences arising from the use of any information it contains.

ROYAL SOCIETY OF CHEMISTRY

rsc.li/dalton

View Article Online
DOI: 10.1039/D0DT01340D

RSCPublishing

COMMUNICATION

Received 00th XXXX 2019,
Accepted 00th XXXX 2019

DOI: 10.1039/c9ccxxxxxx

# Self-assembly of mixed-valent and heterometallic metallocycles: efficient catalyst for oxidation of alcohols to aldehydes with ambient air

Ya-Liang Lai, Xue-Zhi Wang, Rui-Rong Dai, Yong-Liang Huang, Xian-Chao Zhou, Xiao-Ping Zhou* and Dan Li

**Two mixed-valent $Cu^{II}/Cu^{I}$ and two heterometallic $Cu^{II}/Ag^{I}$ metallocycles have been synthesized by the assembly of designed metalloligands and $Cu^{I}/Ag^{I}$ ions, respectively. The $Cu^{II}/Cu^{I}$ metallocycle can catalyze oxidation of alcohols to aldehydes mediated by co-catalyst TEMPO (2,2,6,6-tetramethylpiperdine-1-oxyl) with ambient air as oxidant, while $Cu^{II}/Ag^{I}$ metallocycle has no catalytic effect.**

The design and construction of discrete supramolecular coordination complexes (SCCs) including metallocycles and coordination cages through coordination driven self-assembly have attracted gigantic attentions for their aesthetically pleasing structures and advanced functions (e.g. host-guest chemistry, [1, 2] catalysis, [3, 4] optical materials,[5-7] bioengineering [8]). Metallocycles are large metal-organic rings in which metal ions bind with organic ligands through dative bonds. Due to the highly directional and relatively strong dative bonds, the metallocycles can be designed and prepared with predictable shapes and sizes. A huge number of metallocycles have been successfully synthesized with varied geometries (e.g. triangles, squares or rectangles, pentagons, hexagons, heptagon, and octagon).[9-11] In these metallocycles, the electronic state and coordination geometry of metal ions may play critical roles in both structures and functions. The metallocycle with mixed-valent or heterometallic metal ions is important, [3] as the different metal centers can probably act either as structural nodes or functional sites. However, the self-assembly of metallocycles featuring identical structure with mixed-valent and heterometallic metal ions is unusual, in which precisely designed building unit is required for binding with different types of metal ions.

*College of Chemistry and Materials Science, Jinan University, Guangzhou, Guangdong 510632, P. R. China. E-mail: zhouxp@jnu.edu.cn*

† Electronic supplementary information (ESI) available: Experimental section, characterization and physical measurements. CCDC Nos. 1963369-1963370, 1974814-1974815. See DOI: 10.1039/xxxxxxx

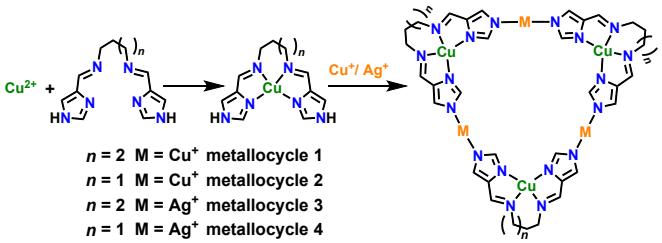


**Scheme 1.** Schematic representation of stepwise synthesis of metallocycles **1-4**

A complex that has appended functional binding sites to coordinate to additional metal ions, is regarded as a metalloligand. Metalloligands have been employed in the self-assembly of metallocycles via a stepwise synthesis,[12, 13] which is documented as a useful approach, especially for heterometallic metallocycles.[3] In our previous studies, we found that a mononuclear metal complex based on bis-imidazole ligand with Schiff base groups can act as a metalloligand (Scheme 1 and Fig. S1 ESI†), which have been employed as the building unit to construct coordination cages and coordination polymers.[14, 15] We hypothesized this metalloligand can be probably used as a building unit for metallocycles: 1) The mononuclear metal complex contains two convergent unbinding sites (<N-Cu-N ≈ 98 °, Fig. S1, ESI†); 2) the soft nitrogen in imidazole ligand can bind with soft linear coordinated coin metal ions (e.g. $Cu^{I}$ and $Ag^{I}$); 3) previous reports have shown that the imidazole ligand can form metallocycles with coin metal ions.[10] Herein, we report the stepwise construction of two mixed-valent $Cu^{II}/Cu^{I}$ and two heterometallic $Cu^{II}/Ag^{I}$ metallocycles by using two copper(II)-imidazolate complexes as a metalloligand (Scheme 1). Both the mixed-valent and metallocycles have identical triangular structures. Interestingly, we found that the $Cu^{II}/Cu^{I}$ metallocycle shows excellent catalytic activity on the oxidation of alcohol mediated by TEMPO, whereas there is no catalytic effect for heterometallic $Cu^{II}/Ag^{I}$ metallocycle. Furthermore, the $Cu^{II}/Cu^{I}$ metallocycle can be further used to catalyze the Knoevenagel condensation of benzaldehyde and malononitrile to achieve a sequential catalysis.

Ligands $H_2L1$ (*N*,*N*'-(butane-1,4-diyl)bis(1-(1H-imidazol-4-yl)methanimine) and $H_2L2$ (*N*,*N*'-(propane-1,3-diyl)bis(1-(1H-

imidazol-4-yl)methanimine)) were synthesized from the condensation of 4-formylimidazole with corresponding diamine molecules (1,4-diaminobutane for $H_2L$ and 1,3-diaminopropane for $H_2L2$). [14] Then, the mononuclear complexes $Cu(H_2L1)$ and $Cu(H_2L2)$ were obtained by reacting the $H_2L1$ and $H_2L2$ with $Cu(ClO_4)_2{\cdot}6H_2O$, respectively. Finally, the reacting metalloligands ($Cu(H_2L1)$ and $Cu(H_2L2)$) with $Cu_2O/AgNO_3$ in mixed solvents (*N*, *N*'-dimethylacetamide (DMA)/ ethanol, 2:1, v/v) at 100 °C for 72 h afforded four metallocycles (see the ESI† for details), formulated as $Cu^{I}_3(Cu^{II}L1)_3{\cdot}3ClO_4$ (**1**), $Cu^{I}_3(Cu^{II}L2)_3{\cdot}3ClO_4$ (**2**), $Ag^{I}_3(Cu^{II}L1)_3{\cdot}3NO_3$ (**3**), and $Ag^{I}_3(Cu^{II}L2)_3{\cdot}3NO_3$ (**4**), respectively. Single crystals of metallocycles **1-4** were obtained in the solvothemal processes. Further studies found that metallocycles **1-4** can also be synthesized in one step by mixing the ligands and metal salts under similar conditions (Scheme S1, see ESI† for details).

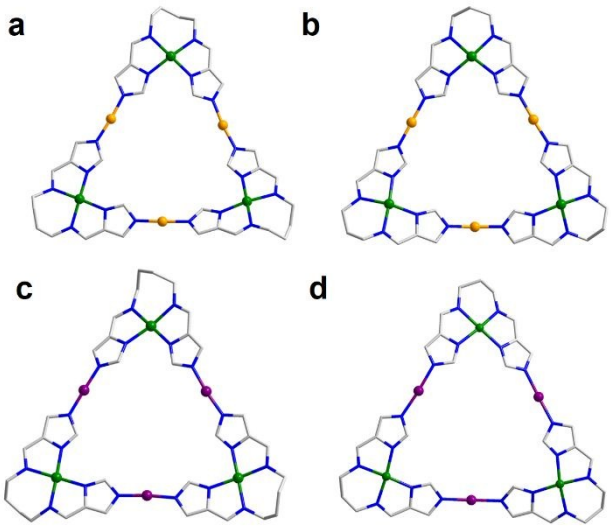


**Fig. 1** Crystal structures of metallocycles **1** (a), **2** (b), **3**(c), and **4** (d). Color codes: $Cu^{II}$, Green; $Cu^{I}$, orange; $Ag^{I}$, purple; C, light gray; N, blue. All hydrogen atoms and anions are omitted for clarity.

Single-crystal X-ray diffraction (SCXRD) analysis revealed that all the crystals of metallocycles **1-4** crystalize in a $P\bar{1}$ space group, featuring similar hexanuclear triangular structures (Fig. 1). The structure of metallocycle **1** will be described in detail as an example. Due to the low symmetry, the asymmetric unit in **1** contains one triangular metallocycle composed of 6 copper centres and 3 ligands and three $ClO_4^-$ anions to balance the positive charges (Fig S2, ESI†). As shown in Fig. 1a, there are two types of copper centers in **1**. The first one probably has an oxidation state of +2, where $Cu^{II}$ was chelated by ligand L1 to form a copper(II)-imidazolate metalloligand. The second one should have an oxidation state of +1, which $Cu^{I}$ links the metalloligands to form a triangular metallocycle. Two $Cu^{II}$ centers adopt five-coordinated (four nirtrogen from the ligand, one oxygen from $ClO_4^-$) square pyramidal geometry and one $Cu^{II}$ adopts a four-coordinated square planar geometry (four nirtrogen from ligand), while the $Cu^{I}$ adopts a linear coordination geometry (<N-Cu-N, 171.788 – 175.313 °). The $Cu^{II}$-N bond distances were in the range of 1.976 - 2.026 Å, while the $Cu^{II}$ -O bond distances were obviously longer (2.452 – 2.524 Å) due to a Jahn–Teller effect for copper centers. The $Cu^{II}$-N bond distances are longer than that of $Cu^{I}$-N bond distances (1.857 -1.868 Å), which is in good agreement with the reported mixed-valent $Cu^{II}/Cu^{I}$ complexes. [16, 17] L1 coordinates with one $Cu^{II}$ ions and two $Cu^{I}$ ions in **1**, bridging the metal centers to construct metallocycle **1**. The $Cu^{II}\cdots Cu^{II}$ distances in metallocycle **1** were 11.594, 11.678, and 11.724 Å, respectively, while that of $Cu^{I}\cdots Cu^{I}$ were 7.687, 8.021, 8.181 Å, respectively. The cavity of metallocycle **1** is occupied by a $ClO_4^-$ anion (Fig. 2a), as the guest. Due to the $ClO_4^-$ anion binding on the $Cu^{II}$, an inter-threading supramolecular dimer is formed, as shown in Fig. 2b. Although the metallocycles with triangular structure have been reported previously, to our best knowledge, the assembly of two metallocycles by threading to form a supramolecular dimer is firstly observed.

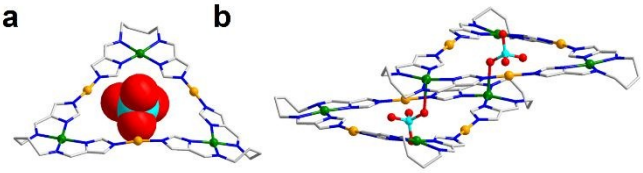


**Fig. 2** Crystal structure of metallocycle **1** filled with $ClO_4^-$ anion (a) and the structure of inter-threading supramolecular dimer (b). Color codes: $Cu^{II}$, Green; $Cu^{I}$, orange; C, light gray; N, blue; O, red; Cl, turquoise; H, omitted.

The structure of metallocycle **2** is similar to **1**, in which the L1 is replaced with L2. The $Cu^{II}\cdots Cu^{II}$ distances (11.519-11.605Å) in metallocycle **2** were lightly shorter than that of **1** (11.594 - 11.724 Å), while its $Cu^{I}\cdots Cu^{I}$ distances (8.167 – 8.230 Å) were lightly longer than that of **1** (7.687 - 8.181 Å). By replacing the $Cu^{I}$ with $Ag^{I}$, similar metallocycles **3** and **4** were obtained (Figs. 1c and d), respectively. However, both the $Cu^{II}\cdots Cu^{II}$ distances in **3** (11.961 – 12.177 Å) and **4** (11.870 – 12.068 Å) were longer than that of **1** and **2**, which was probably due to their longer Ag-N coordination bond distances (2.060 – 2.116 Å). Interestingly, both the metallocycles **3** and **4** selectively host the $NO_3^-$ anions as the guests (Fig. S3 ESI†), although the same amount of $ClO_4^-$ anion also presented in the reaction mixture.

Powder X-ray diffraction (PXRD) analysis showed that the PXRD patterns of metallocycles **1-4** closely matched with their simulated ones from SCXRD data, indicating that the pure phase of these metallacycles can be obtained (Figs. 3a and b, Fig. S4 ESI†). To confirm the mixed valence state of copper centers in metallocycles **1** and **2**, X-ray photoelectron spectra (XPS) of **1** and **2** were measured. As shown in Figs. 3c and d, intense asymmetrical Cu $2p_{3/2}$ photoelectron peaks with satellite peaks are presented in both spectra, indicating the mixed-valent feature of copper centers in **1** and **2**.[18, 19] The Cu $2p_{3/2}$ peaks can be deconvoluted into two contributions located at 933.04 and 934.89 eV for **1** (Fig. 2c) and 932.87 and 934.59 eV for **2** (Fig. 2d), corresponding to the $Cu^{I}$ and $Cu^{II}$ species in peak area ratios of approximately 3 : 2 and 2 : 3, respectively. The peak area ratio of $Cu^{I}$ and $Cu^{II}$ of XPS results is not in agreement with the crystal structure. The possible reason is that the XPS is surface-sensitive quantitative technology. On the other hand, bond valence sum (BVS) has been used to determine the oxidation state of metal ions based on their metal-ligand bond

distances in SCXRD structure or extended X-ray absorption fine structure (EXAFS).[20] The calculation of BVS values for the three $Cu^{II}$ centers in **1** gives 2.037, 2.043, and 2.031, respectively, while that of three $Cu^{I}$ centers gives 0.981, 0.964, and 0.958, respectively. Similarly, the BVS of three $Cu^{II}$ centers in **2** are 2.068, 2.105, and 2.088, respectively, while that of three $Cu^{I}$ centers are 0.978, 0.976, and 0.990, respectively. All these BVS values are in good agreement with the results of SCXRD and XPS, proving the mixed-valent property of both metallocycles **1** and **2**

Mass spectrometry was usually employed for checking the solution states of cages and metallocycles. The high-resolution mass spectra of metallocycles **1**-**4** were measured by an electrospray ionization time-of-flight mass spectrometer (ESI-TOF-MS) in acetonitrile. As shown in Fig. S5 (ESI†), the main cationic peaks arise mainly from the broken species of metallocycles (e.g. $[CuL1\text{-}H]^+$, $[Cu_3L_2\text{-}4H]^+$ in spectrum of **1**), indicating that metallocycles **1**-**4** are probably not stable under the ESI-TOF-MS measurement. However, we can find some weak cationic peaks arising from the loss of anions and hydrogen from the metallocycles (such as m/z 603.395, $[Cu_3(CuL1)_3(ClO_4)\text{-}6H]^{2+}$ for **1**, 582.695, $[Cu_3(Cu_3L2)_3(ClO_4)\text{-}6H]^{2+}$ for **2**, 620.594 $[Ag_3(CuL1)_3\text{-}7H]^{2+}$ for **3**, 630.530, $[Ag_3(CuL2)_3(NO_3)\text{-}6H]^{2+}$ for **4**) in the spectra, suggesting that metallocycles **1**-**4** should exist in acetonitrile solution.

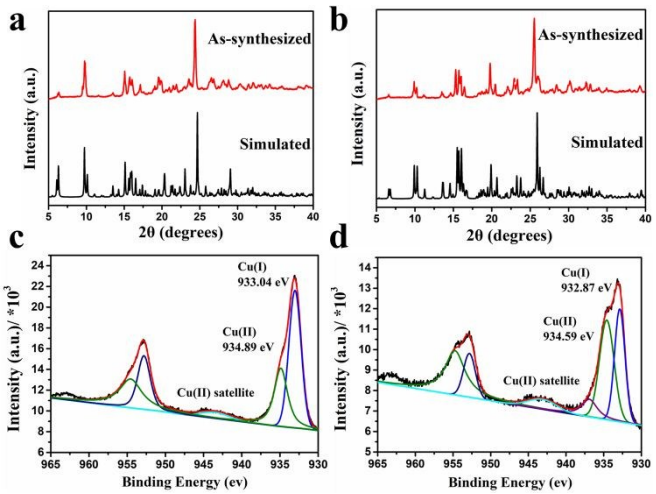


**Fig. 3** PXRD patterns of **1** (a) and **2** (b), and XPS spectra of **1** (a) and **2** (d) with fitting peaks (blue $Cu^{I}$, green $Cu^{II}$).

Aldehydes act as important roles in organic reactions and high-value components in the perfume industry. They can be produced from the oxidation of alcohols by employing stoichiometric amounts of inorganic oxidizing reagents, including chromium and manganese oxides.[21] Such oxidization reactions are poorly selective and generate copious amounts of heavy-metal waste, which are not environmentally friendly. Therefore, the development of green catalysis for oxidation of alcohols by using green oxidizing reagents (e.g. $O_2$) seems highly desirable and is fundamentally important in laboratory and industrial settings.[22] The galactose oxidase (GO) enzyme containing copper catalytic centres can selectively oxidize primary alcohols to aldehydes. To mimic GO enzyme, copper(I/II) complexes have been employed for catalysing the oxidation of alcohols to aldehydes by combining with a stable nitroxyl radical such as TEMPO and molecular oxygen.[23-25] We hypothesize that the $Cu^{II}/Cu^{I}$ mixed-valent metallocycles can probably act as an efficient catalyst for the aerobic oxidation of alcohols to aldehyde by using TEMPO as co-catalyst.

The solubility of metallocycle **1** is better than **2** in acetonitrile. Thus, the catalytic activity of **1** for the oxidization of alcohol was assessed, and the oxidation of benzyl alcohol was selected as a model reaction. Gas chromatography (GC) results demonstrated that the oxidation of benzyl alcohol into benzyl aldehyde is successful by using metallocycle **1**, TEMPO, *N*-methylimidazole (NMI), and acetonitrile at room temperature with ambient air, in which the TEMPO and NMI acts co-catalyst and base, respectively. After optimization of the reaction parameters, the catalyst system employed here consists of 5 mol% **1**, 10 mol % TEMPO, and 50 mol % NMI in acetonitrile. As shown in Fig. S6 (ESI†), although the reaction rate is slow in the first 40 min, metallocycle **1** could catalyse the oxidation of benzyl alcohol with 99.99 % conversion in 2 hours. The further oxidation benzyl aldehyde to benzoic acid is not observed during the reaction even with longer reaction time, indicating the excellent selectivity of the catalyst. For comparison, the catalytic performance of metallocycle **3** was also accessed under the same conditions. Experimental results showed that trace benzyl aldehyde was detected, indicating that **3** can not catalyse the oxidation of benzyl alcohol to benzyl aldehyde. The structure difference between **1** and **3** is the linear coordination metal ions ($Cu^{I}$ **1**, $Ag^{I}$ **3**), suggesting that the catalytic site for **1** is likely the $Cu^{I}$ centre, than $Cu^{II}$. The possible reason is that $Cu^{II}$ in both **1** and **3** is chelated by L1, which do not have accessible active site to catalyse the benzyl alcohol. Therefore, as proposed by Stahl., et al,[23] the plausible mechanism may contain two important separate half-reactions (Fig. S7). First, the $O_2$ of air oxidize the $Cu^{I}$ and TEMPOH. Second, the yielded intermediated $Cu^{II}$ species oxidize the alcohol to aldyhyde, which is mediated by TEMPO.

Inspired by the good catalytic performance of metallocycle **1** for the oxidation of benzyl alcohol into benzyl aldehyde under ambient conditions, the scope of this oxidation reaction was further explored. As shown in Fig. 4, 16 aromatic alcohol molecules with various substitutional groups and heteroaromatic alcohols were tested. Both electro-withdrawing and -donating substitutional groups on the benzene ring of benzyl alcohols were well-tolerated (conversion > 99.9 %). On the other hand, the heteroaromatic alcohols including 2-furylmethanol, 2-thienylmethanol, and 3-pyridinylmethanol also afford excellent conversion (> 99.9%) in 2 h. However, for 1-naphthalenemethanol, the conversion (~ 70%) is obviously lower than that of 2-naphthalenemethanol, which is probably due to its steric hindrance.

Due to metallocycle **1** also contains weak base groups (e.g. imidazole and Schiff base groups), it can probably catalyze the Knoevenagel condensation reaction.[26] Thus, the sequential alcohol oxidation/Knoevenagel condensation reaction can probably be reached by employing **1** as catalyst (Scheme S2, ESI†). Upon the completion of oxidation of benzyl alcohol, malononitrile (2.0 equiv.) was added to the reaction mixture. The product

benzylidenemalononitrile was acquired in 90.0 % conversion after 1.5 h. The sequential reaction afforded an extremely low conversion (< 2%) without add **1** as catalyst. This preliminary result showed that metallocycle **1** can be used as a potential catalyst for sequential reactions.

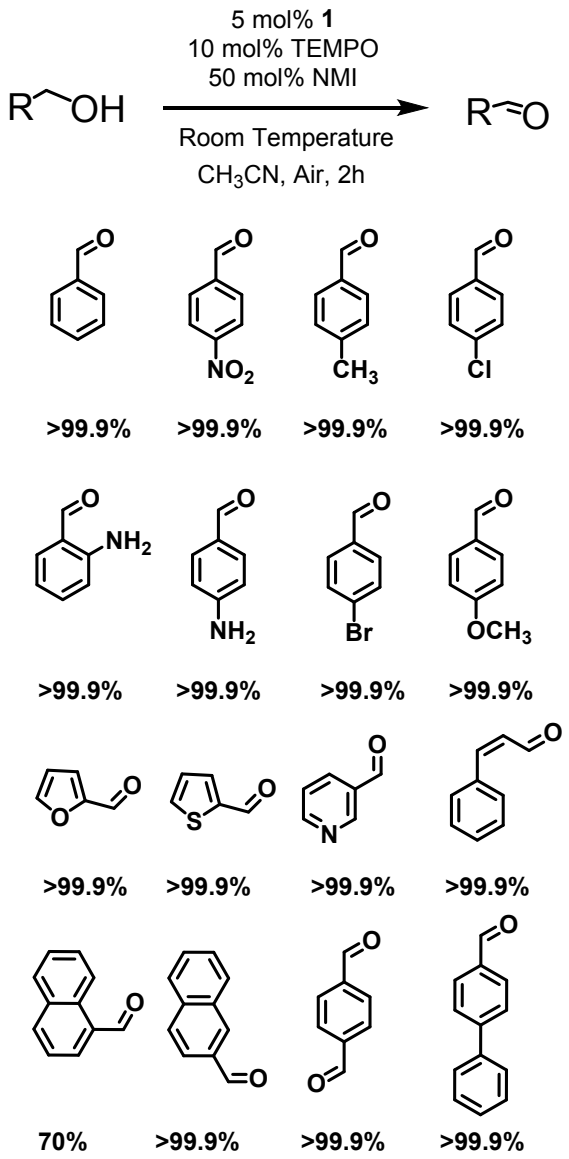


**Fig. 4** The oxidation of various aromatic alcohols over metallocycle **1**.

In summary, we have successfully constructed two mixed-valent $Cu^{II}/Cu^{I}$ and two heterometallic $Cu^{II}/Ag^{I}$ metallocycles by using the metalloligand approach. These metallocycles feature similar triangular structures. Interesting inter-threading supramolecular dimers were observed between two adjacent metallocycles with their binding anions. Metallocycle **1** is an efficient catalyst for oxidation aromatic alcohols to aldehyde. Furthermore, metallocycle **1** can catalyze the Knoevenagel condensation reaction, providing a potential material for sequential catalysis. This work provides a good strategy for designing mixed-valent and heterometallic metallocycles. It can be expected that these interesting metallocycles can be employed as catalyst for more organic reaction.

This work was supported by the National Natural Science Foundation of China (Nos. 21731002, 21871172, 21801095), the Major Program of Guangdong Basic and Applied Research (No. 2019B030302009), the Fundamental Research Funds for the Central Universities (21619405), and Jinan University.

## Conflicts of interest

There are no conflicts to declare.

## Notes and references

1. F. J. Rizzuto, L. K. S. von Krbek and J. R. Nitschke, *Nat. Rev. Chem.*, 2019, **3**, 204-222.
2. X. Zhang, X. Dong, W. Lu, D. Luo, X.-W. Zhu, X. Li, X.-P. Zhou and D. Li, *J. Am. Chem. Soc.*, 2019, **141**, 11621-11627.
3. W.-X. Gao, H.-N. Zhang and G.-X. Jin, *Coord. Chem. Rev.*, 2019, **386**, 69-84.
4. J. Wei, L. Zhao, C. He, S. Zheng, J. N. H. Reek and C. Duan, *J. Am. Chem. Soc.*, 2019, **141**, 12707-12716.
5. W. Xuan, M. Zhang, Y. Liu, Z. Chen and Y. Cui, *J. Am. Chem. Soc.*, 2012, **134**, 6904-6907.
6. M. L. Saha, X. Yan and P. J. Stang, *Acc. Chem. Res.*, 2016, **49**, 2527-2539.
7. J.-P. Lang, Q.-F. Xu, Z.-N. Chen and B. F. Abrahams, *J. Am. Chem. Soc.*, 2003, **125**, 12682-12683.
8. H. Sepehrpour, W. Fu, Y. Sun and P. J. Stang, *J. Am. Chem. Soc.*, 2019, **141**, 14005-14020.
9. S. Leininger, B. Olenyuk and P. J. Stang, *Chem. Rev.*, 2000, **100**, 853-908.
10. X.-C. Huang, J.-P. Zhang and X.-M. Chen, *J. Am. Chem. Soc.*, 2004, **126**, 13218-13219.
11. T. Zhang, L. P. Zhou, X. Q. Guo, L. X. Cai and Q. F. Sun, *Nat Commun*, 2017, **8**, 15898.
12. W.-H. Zhang, Z.-G. Ren and J.-P. Lang, *Chem. Soc. Rev.*, 2016, **45**, 4995-5019.
13. X.-T. Qiu, R. Yao, W.-F. Zhou, M.-D. Liu, Q. Liu, Y.-L. Song, D. J. Young, W.-H. Zhang and J.-P. Lang, *Chem. Commun.*, 2018, **54**, 4168-4171.
14. X.-Z. Wang, M.-Y. Sun, J. Zheng, D. Luo, L. Qi, X.-P. Zhou and D. Li, *Dalton Trans.*, 2019, **48**, 17713-17717.
15. Y.-L. Hou, Y. Pi, X.-P. Zhou and D. Li, *Inorg. Chem.*, 2018, **57**, 2377-2380.
16. W.-X. Ni, M. Li, X.-P. Zhou, Z. Li, X.-C. Huang and D. Li, *Chem. Commun.*, 2007, 3479-3481.
17. X.-C. Huang, J.-P. Zhang, Y.-Y. Lin, X.-L. Yu and X.-M. Chen, *Chem. Commun.*, 2004, 1100-1101.
18. D. C. Frost, A. Ishitani and C. A. McDowell, *Mol. Phys.*, 1972, **24**, 861-877.
19. S. Zhang and L. Zhao, *Nat. Commun.*, 2019, **10**, 4848.
20. H. H. Thorp, *Inorg. Chem.*, 1992, **31**, 1585-1588.
21. G.-J. t. Brink, I. W. C. E. Arends and R. A. Sheldon, *Science*, 2000, **287**, 1636-1639.
22. Y.-Z. Chen, Z. U. Wang, H. Wang, J. Lu, S.-H. Yu and H.-L. Jiang, *J. Am. Chem. Soc.*, 2017, **139**, 2035-2044.
23. J. M. Hoover, B. L. Ryland and S. S. Stahl, *J. Am. Chem. Soc.*, 2013, **135**, 2357-2367.
24. J. M. Hoover and S. S. Stahl, *J. Am. Chem. Soc.*, 2011, **133**, 16901-16910.
25. J. M. Hoover, J. E. Steves and S. S. Stahl, *Nat. Protoc.*, 2012, **7**, 1161-1166.
26. Y. Y. Li, T.-Y. He, R.-R. Dai, Y.-L. Huang, X.-P. Zhou, T. Chen and D. Li, *Chem. Asian J.*, 2019, **14**, 3682-3687.

Communication
View Article Online
DOI: 10.1039/D0DT01340D

**For TOC**